Dynamics-Aware and Beamforming-Assisted Transmission for Wireless Control Scheduling

Ling Lyu, *Student Member, IEEE*, Cailian Chen, *Member, IEEE*, Shanying Zhu, *Member, IEEE*, Nan Cheng, *Member, IEEE*, Yujie Tang, *Student Member, IEEE*, Xinping Guan, *Fellow, IEEE*, and Xuemin Shen, *Fellow, IEEE*

***Abstract*— The wide application of Internet of Things (IoT) in industrial automation leads to the emergence of a new paradigm of industrial IoT systems, namely wireless control system, where control commands are transmitted from the remote controller to multiple actuators over shared wireless channels. Considering system stability, distinct subsystems usually have different requirements on the transmission quality of control commands due to different system dynamics. In this paper, we aim to simultaneously guarantee the stability of all subsystems and minimize the weighted sum of control cost and transmission cost. To this end, the maximum tolerated packet loss rate of each subsystem is first characterized by a pre-defined Lyapunov function. Then, based on channel conditions and system dynamics, a beamforming-assisted hierarchical coordinated transmission strategy is proposed to alleviate the impact of unreliable transmission on the control performance. The control performance and energy efficiency are further optimized by formulating an overall cost minimization problem constrained by the system stability. Both the differential accumulation and the difference-convex methods are employed to effectively deal with the constraint that is expressed in an implicit probabilistic form. Finally, simulation results demonstrate that the proposed strategy has the advantages of reducing control cost and energy consumption.**

***Index Terms*— Industrial IoT, wireless control systems, transmission reliability, system stability, beamforming.**

I. Introduction

INTERNET of Things (IoT) has been applied in many industries such as manufacturing, oil and gas, energy mining, metals and other industrial sectors [1]–[8]. Recently, the emerging wireless control system (WCS) is regarded as a typical paradigm of industrial IoT in the application of intelligent manufacturing, which is usually constituted by a multitude of small-scale integrated subsystems. In addition, WCS generally has the ability to collect a large amount of data and convert the data into useful information. In the multi-subsystem WCS, the separation of control and actuation involves the data transmission of control commands over shared wireless channels. In general, the more information the controller sends, the more precise actuation becomes, leading to that the control performance improves at the cost of more energy and spectrum resources. In this paper, we aim to minimize the overall cost for multi-subsystem WCS, while meeting the stability condition required by control system with limited communication resources.

In the past decade, the communication-constrained control has been widely investigated in the area of networked control [9]–[14]. In order to guarantee the system stability and improve control performance, the control-scheduling strategy is adjusted based on system dynamics, while satisfying the resource constraint imposed by the communication network. Taking the packets loss and/or transmission delay into account, many existing studies [15]–[18] adopt the switching system approach to analyze the system stability with static scheduling protocols. Moreover, as the subsystem with higher dynamics has the larger demand to be scheduled, some dynamic scheduling strategies have been proposed to determine the scheduled probability for each subsystem [19], [20].

Besides designing the control-scheduling strategy based on system dynamics, another important issue is how to successfully complete data transmissions for the scheduled subsystems over lossy wireless channels. However, in these aforementioned studies, the assumption about the perfect communication of control commands is over ideal. In practice, the harsh industrial wireless environments, such as electromagnetic interference, high temperature and humidity levels, vibrations, dirt, and dust, may result in the uncertain and stochastic wireless channels [21]–[23]. How to achieve a reliable and efficient data transmission with poor channel conditions has attracted a lot of attention from both academia and industry. Traditional techniques to enhance the reliability of wireless communications, such as retransmission and redundancy [24], focus on transmitting additional packets or bits to achieve the loss-recovery. A price we need to pay, however, is the increasing time delay and energy consumption. Thus, they are not suitable for the delay-sensitive and energy-limited

Manuscript received March 19, 2018; revised July 5, 2018 and August 25, 2018; accepted August 27, 2018. Date of publication September 18, 2018; date of current version November 9, 2018. This work was supported in part by the NSF of China under Grants 61521063, 61622307, 61633017, U1405251, 61371085, 61603251, and U1509211, in part by NSF of Shanghai under Grant 18ZR1419900, and in part by the China Scholarship Council. The associate editor coordinating the review of this paper and approving it for publication was K. Choi. *(Corresponding author: Cailian Chen.)*

L. Lyu, C. Chen, S. Zhu, and X. Guan are with the Department of Automation, Shanghai Jiao Tong University, Shanghai 200240, China, and also with the Key Laboratory of System Control and Information Processing, Ministry of Education of China, Shanghai 200240, China (e-mail: sjtulvling@sjtu.edu.cn; cailianchen@sjtu.edu.cn; shyzhu@sjtu.edu.cn; xpguan@sjtu.edu.cn).

N. Cheng is with the School of Telecommunication Engineering, Xidian University, Xi'an 710071, China (e-mail: n5cheng@uwaterloo.ca).

Y. Tang and X. Shen are with the Department of Electrical and Computer Engineering, University of Waterloo, Waterloo, ON N2L 3G1, Canada (e-mail: y59tang@uwaterloo.ca; sshen@uwaterloo.ca).

Color versions of one or more of the figures in this paper are available online at http://ieeexplore.ieee.org.

Digital Object Identifier 10.1109/TWC.2018.2869589

industrial IoT applications [25]. When the time diversity is not viable in the delay-sensitive scenario, exploiting the spatial diversity is a real choice to improve the transmission reliability for industrial automation systems [26]. Swamy *et al.* [26] has proposed a wireless communication protocol that capitalizes on multiuser diversity and cooperative communication to achieve the ultra-reliability with a low-latency constraint. The beamforming technique [27] has been regarded as a promising solution to improve transmission reliability. In general, joint beamforming and coordinated beamforming are two common methods used to manege interference. In [28], the joint beamforming cancels interferences by converting a potential interferer to desired signals, which is achieved at the cost of overwhelming overhead introduced by signals sharing. In [29], the coordinated beamforming adjusts the corresponding beamformers in a coordinated way to mitigate the excessive interference. However, the achieved transmission capacity and spectrum utilization are worse than that with the former one.

For control applications in industrial IoT with multiple subsystems, subsystems with different dynamic characteristics have distinct impacts on guaranteeing the stability and reducing the overall control cost of whole system. To solve such problem, we aim to design a reliable and efficient transmission strategy to guarantee the system stability and reduce the overall cost. To this end, a dynamics-aware and beamforming-assisted two-tier coordinated transmission strategy is proposed for multi-subsystem WCSs to reduce the transmission outage probability of control commands. Specifically, in the considered multi-subsystem WCS, the control commands are transmitted from the multi-antenna controller to multiple single-antenna actuators via multiple single-antenna assisted devices (ADs). ADs in charge of forwarding received packets are grouped into clusters based on the information of delivered packets. Unfortunately, the limited transmission capacity between the remote controller and ADs makes each AD successfully receive only a part (not all) of actuators' packets, namely only a subset of ADs can participate in the coordination transmission for each actuator. Considering the performance-overhead tradeoff, intra-cluster ADs work with joint beamforming to improve the transmission performance, while the coordinated beamforming is used by inter-cluster ADs to mitigate interference and reduce overhead. The contributions of this paper are summarized as follows.

- The lower bound of the successful transmission probability of control commands is derived to explicitly characterize the relationship between system stability and transmission reliability;
- We propose a coordinated transmission strategy to balance the transmission reliability and the resource limitation, which is achieved by jointly designing the beamforming vector, channel allocation and power control;
- We formulate a system stability constrained optimization problem to minimize the weighted sum of plant regulation cost and information transmission cost. Moreover, the constraint expressed in the implicit probabilistic form is effectively handled with differential accumulation and difference-convex methods.

TABLE I
SYMBOLS AND ABBREVIATIONS

$\mathbb{1}\{\circ\}$	Indicator function	WCS	Wireless Control System
$\|\circ\|$	Norm operation	AD	Assisted Device
$\mathbb{E}\{\circ\}$	Expectation operation	LQG	Linear Quadratic Gaussian
$\Pr\{\circ\}$	Probability operation	SNR	Signal to Noise Ratio
$\mathrm{diag}(\circ)$	Diagonal matrix operation	SINR	Signal to Interference plus Noise Ratio
$\mathcal{S}$	Set of ADs	$a_{m,k}$	Channel $k \in \mathcal{K}$ is assigned to user $m \in \mathcal{M}$
$\mathcal{M}$	Set of subsystems	$\mathbf{g}_s[k]$	Channel vector between controller and AD s on subcarrier k
$\mathcal{K}$	Set of subcarriers	$\mathbf{v}_s[k]$	Precoding vector between controller and AD s on subcarrier k
ΔF	Bandwidth of each subcarrier	P_C	Maximum transmission power of remote controller
F_t	Bandwidth assigned for top tier	P_s	Maximum transmission power of AD s
F_b	Bandwidth assigned for bottom tier	$\mathbf{h}_m$	Channel state information vector from all ADs to actuator m
$\mathbf{x}$	State vector	$\mathbf{w}_m$	Transmit beamformer vector from all ADs to actuator m
$\mathbf{u}$	Calculated control input	β	Control command losses or not
$\hat{\mathbf{u}}$	Actually executed control input	$\mathcal{K}_m$	Set of subcarriers used for transmitting actuator m's data
ζ	System noise	$\mathcal{S}_m$	Set of ADs selected for delivering data of actuator m
A	State transition matrix	$\overline{\mathcal{S}}_m$	Set of ADs not selected for delivering data of actuator m
B	Input matrix	$\Gamma^t_{m,s}[k]$	Received signal SNR of actuator m at AD s on subcarrier k
Ξ	Noise covariance matrix	$R^t_{m,s}$	Achievable rate of actuator m in the top-tier transmission process
$\mathcal{J}$	LQG control cost	Γ^b_m	SINR of signal received by actucator m
$\Delta\mathcal{J}$	Execution deviation	R^b_m	Achievable rate of actuator m in the bottom-tier transmission process

The remainder of this paper is organized as follows. In Section II, the communication network and control system models are presented. In Section III, a dynamics-aware and beamforming-assisted reliable transmission strategy is proposed. In Section IV, we investigate the joint optimization of control scheduling and transmission strategy under the condition of system stability. Simulation results and main conclusions are given in Section V and Section VI, respectively. Table I summarizes the key symbols and abbreviations used in this paper.

II. System Models

In the considered multi-subsystem WCS, the dynamics of different subsystems are generally different, which makes the control inputs of different subsystems different. In this case, different actuators usually execute different control commands to stabilize their own subsystems. Thus, we consider the architecture that the remote controller transmits many independent control signals to many independent actuators. We consider a WCS consisting of multiple independent subsystems that share wireless channels. Each control subsystem consists of one sensor-actuator pair, whose feedback control commands are transmitted from the remote controller to actuators via multiple ADs, as shown in Fig. 1. The solid lines show wired connection.[1] It is practically feasible to employ the beamforming technique in the considered scenario, where

[1]For the considered industrial application, the high-temperature and high-humidity plant makes the cables easily be corroded. Taking the rolling system for example, we usually use the non-contacted method to measure and estimate the slab temperature, such as the infrared imagery of the slab and the temperature of the cooling water. Therefore, the sensor data could be transmitted to the controller by wired networks (such as the fieldbus in industrial automation). However, the actuators and the controlled plant are generally gathered together, thus the actuators wirelessly communicate with the remote controller. Similar to [19], the sensors are wired connected to remote controller, while the actuators receive control command through shared wireless channels.

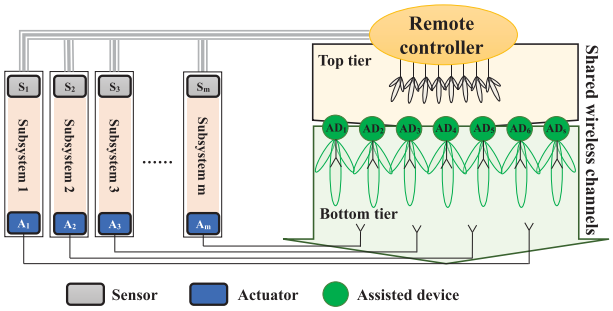

Fig. 1. Multi-subsystem WCS for industrial IoT applications.

a static network with multiple ADs distributed in space is deployed to support the industrial IoT applications [30]–[32]. By taking the unreliable transmission imposed by the lossy wireless channels into account, the remote controller is in charge of jointly optimizing the control scheduling and the transmission strategy, which is beneficial to guarantee the stability of each subsystem constrained by limited spectrum and energy resources.

A. Wireless Communication Model

The wireless communication network providing services for control applications includes one N-antenna remote controller, a set of single-antenna ADs, $\mathcal{S}$, and a set of sensor-actuator pairs, $\mathcal{M}$. The data packet containing the control command is delivered from the remote controller to actuators via multiple ADs, and thus the whole transmission process includes two sub-processes. SubPhase-I is the data transmission from the remote controller to multiple ADs (referred to as top-tier transmission process). SubPhase-II is the data transmission from ADs to actuators (referred to as bottom-tier transmission process). In order to avoid the severe interference between the two sub-processes, the two-tier transmission considered in this paper works on the frequency division duplex mode[2] by sharing all available bandwidth $\mathcal{F}$. For expression simplicity, the bandwidth of each subcarrier is denoted as ΔF, and the bandwidth occupied by the top-tier and the bottom-tier transmission is F_t and F_b, respectively. Throughout this paper, the channel gains of all channels are independent and assumed to follow the Rayleigh block-fading model.

B. Control System Model

The discrete-time linear model for the considered m-th subsystem is expressed as

$$\mathbf{x}_{t+1}^m = A_m \mathbf{x}_t^m + B_m \mathbf{u}_t^m + \zeta_t^m, m \in \mathcal{M}, \tag{1}$$

where $\mathbf{x}_t^m \in \mathbb{R}^{\kappa_x}$ is the state vector, $\mathbf{u}_t^m \in \mathbb{R}^{\kappa_u}$ is the control input of m-th actuator; $A_m \in \mathbb{R}^{\kappa_x \times \kappa_x}$ is the state transition matrix, and $B_m \in \mathbb{R}^{\kappa_x \times \kappa_u}$ is the input matrix for each actuator $m \in \mathcal{M}$. The initial state $\mathbf{x}_0^m$ is a Gaussian random vector with the covariance matrix $W_0^m > 0$. The system noise $\zeta_t^m \in \Re^{\kappa_x}$ are independent and Gaussian with zero mean and covariance matrix $\Xi_t^m \succ 0$. We consider that the state measurement $\mathbf{x}_t^m$ at time t is able to be collected by sensors and received by the remote controller. Then, the control input $\mathbf{u}_t^m$ is obtained by employing a linear feedback control strategy [33]. Furthermore, we assume that the controller is closed to sensors but far from actuators, see in Fig. 1. As a result, it is reasonable to consider that the transmission between sensors and the controller is perfect without dropping any state measurements, while the data transmission of control commands may fail [34].

[2]For other communication scenarios (such as the time division duplex mode), the design, analysis and optimization method given in this paper is still applicable. In order to avoid the severe interference between the top-tier and the bottom- tier transmission processes, the proposed method requires that all resources are divided into two non-overlapping portions no matter in the frequency domain or in the time domain. In the time division duplex mode, the duration of one time slot in the time division mode is denoted as $T = T_t + T_b$., where T_t and T_b are the top-tier and the bottom-tier transmission time, respectively. All available bandwidth $\mathcal{F}$ is reused by the top-tier and the bottom-tier processes.

III. Dynamics-Aware and Beamforming-Assisted Reliable Transmission Strategy

We aim to reduce the overall cost under the constraint of system stability by taking advantage of the spatial diversity. To this end, a dynamics-aware and beamforming-assisted strategy is proposed to enhance the transmission reliability. Specifically, we firstly explore the impact of imperfect wireless transmission on control performance, and then analyze the stability condition for the multi-subsystem WCS with intermittent control commands. Finally, we focus on designing a dynamics-aware two-tier coordinated transmission strategy to improve the transmission reliability by masterfully combining the joint beamforming with power control.

A. Stability Analysis With Intermittent Control Commands

For each subsystem, under perfect transmission, the optimal feedback law is determined by the Linear Quadratic Gaussian (LQG) gain, i.e.,

$$\mathbf{u}_t^m = G_m \mathbf{x}_t^m, \quad m \in \mathcal{M} \tag{2}$$

The feedback gain G_m is given by $G_m = \left(Q_m^x + B_m^{\mathrm{T}} W_m B_m\right)^{-1} B_m^{\mathrm{T}} W_m A_m$, where W_m is the solution of the standard algebraic Riccati equation $W_m = A_m^{\mathrm{T}} W_m A_m + Q_m^u - A_m^{\mathrm{T}} W_m B_m (Q_m^x + B_m^{\mathrm{T}} W_m B_m)^{-1} B_m^{\mathrm{T}} W_m A_m$ [35]. Assume that (A_m, B_m) is controllable and $(A_m, \Xi_m^{\frac{1}{2}})$ is detectable. For the proof of system stability and optimality, the reader can refer to [36]. The packet loss imposed by imperfect wireless transmissions makes it quite challenging to ensure all subsystems receive their corresponding control commands at each time step. A random binary variable with Bernoulli distribution $\beta_{m,t}$ is introduced. When the data packet of the m-th actuator is received successfully, $\beta_{m,t} = 1$. Otherwise, $\beta_{m,t} = 0$. In this paper, we consider to-be-zero strategy. The control command actually executed by the m-th actuator is $\check{\mathbf{u}}_t^m = \beta_{m,t} \mathbf{u}_t^m$.

To characterize the stability of each subsystem, we employ

$$\begin{aligned}
&\mathbb{E}\{\mathcal{U}_m(\mathbf{x}_{t+1}^m)\} \\
&= \mathbb{E}\{(\mathbf{x}_t^m)^{\mathrm{T}} (A_m)^{\mathrm{T}} U_m A_m \mathbf{x}_t^m + (\zeta_t^m)^{\mathrm{T}} U_m \zeta_t^m + \mu_{m,t} (\mathbf{x}_t^m)^{\mathrm{T}} \\
&\quad \times [(A_m - B_m G_m)^{\mathrm{T}} U_m (A_m - B_m G_m) \\
&\quad - (A_m)^{\mathrm{T}} U_m A_m] \mathbf{x}_t^m\},
\end{aligned} \tag{3}$$

where $\mathcal{U}_m(\mathbf{x}_{t+1}^m) = (\mathbf{x}_{t+1}^m)^{\mathrm{T}} U_m \mathbf{x}_{t+1}^m$ is the quadratic Lyapunov function for subsystem m and U_m is positive definite. The subsystem m is stable if its expected Lyapunov function satisfies the following relation

$$\mathbb{E}\{\mathcal{U}_m(\mathbf{x}_{t+1}^m)\} \leq \eta_m \mathbb{E}\{\mathcal{U}_m(\mathbf{x}_t^m)\} + \mathbb{E}\{(\zeta_t^m)^{\mathrm{T}} U_m \zeta_t^m\}, \quad (4)$$

which indicates that the Lyapunov-like function of system state eventually if $\eta_m < 1$. For each subsystem, integrating (3) with (4), we can obtain (5), shown at the top of next page.
The lower bound of $\mu_{m,t}$, which ensures that all subsystems are stable, could be obtained by solving the optimization problem (6), shown at the top of next page.
which is a semi-definite programming. The optimal value $\mu_{m,t}^{low}$ could be gotten with CVX [37].

We adopt the LQG cost in expectation to assess the control performance of the system

$$\mathcal{J}_m = \mathbb{E}\big\{(\mathbf{x}_T^m)^{\mathrm{T}} Q_m^x \mathbf{x}_T^m + \sum_{t=0}^{T-1} (\mathbf{x}_t^m)^{\mathrm{T}} Q_m^x \mathbf{x}_t^m + (\check{\mathbf{u}}_t^m)^{\mathrm{T}} Q_m^u \check{\mathbf{u}}_t^m\big\}, \quad (7)$$

which relies on both the control performance and the transmission performance. The control objective is to satisfy the stability condition (4) as well as to minimize the control cost (7). It is worthy to note that both the stability condition and the control performance depends on not only the controller design, but also the data transmission reliability.

B. Beamforming Assisted Two-Tier Coordinated Transmission Design

If the control command is lost, this subsystem is open-loop, whose stability can not be guaranteed by adjusting the control law [38]. Motivated by this, we focus on how to improve the transmission reliability to make subsystems be closed-loop by taking full use of the spatial diversity. To this end, we propose a beamforming assisted two-tier coordinated transmission strategy to improve the transmission reliability. Specifically, in the two-tier transmission framework, only a part of ADs participate in the coordination of delivering data packets containing the same control command with joint beamforming technique. Meanwhile, the coordinated beamforming technique is employed to deliver data packets with different control commands from the controller to ADs. The two-tier coordinated transmission is elaborated as follows.

In the top-tier transmission process, let $a_m[k] = 1$ if the data packet of actuator m is assigned to transmit on subcarrier $k \in \mathcal{K}$. Otherwise, $a_m[k] = 0$. Then, the signal-to-noise ratio (SNR) of the received signal at the s-th AD on the k-th subcarrier is given by

$$\Gamma_{m,s}^t[k] = a_m[k] \frac{\left|\mathbf{g}_s[k]\mathbf{v}_s[k]\right|^2}{\sigma_s^t[k]}, \quad (8)$$

where $\sigma_s^t[k]$ is the noise power at AD s on the k-th subcarrier, $\mathbf{g}_s[k]$ is the channel vector between all antennas of remote controller and the s-th AD on the k-th subcarrier, and $\mathbf{v}_s[k]$ is precoding vector between controller and AD s on subcarrier k. For the s-th AD, the achievable data rate of the m-th actuator's control command in the top-tier transmission process is $R_{m,s}^t = \sum_{k\in\mathcal{K}} a_m[k]\Delta F \log(1 + \Gamma_{m,s}^t[k])$. AD s could decode the data packet of the m-th actuator successfully, if the sum rate $R_{m,s}^t(\mathbf{v}, \mathbf{a})$ is not less than the decodable threshold R_{th}^t. This defines the success probability $\Pr\{R_{m,s}^t(\mathbf{v}, \mathbf{a}) \geq R_{th}^t\}$. Another constraint for the top-tier transmission is the maximum transmission power. Let P_C be the maximum transmission power of remote controller, then we have $\sum_{s\in\mathcal{S}} \sum_{k\in\mathcal{K}} \left\|\mathbf{v}_s[k]\right\|_2^2 \leq P_C$. As each subcarrier can only be used to deliver the information of at most one actuator, $\mathbf{1}^{\mathrm{T}}\mathbf{a}[k] \leq 1$, where $\mathbf{a}[k] = [a_1[k], \cdots, a_m[k], \cdots, a_M[k]]^{\mathrm{T}}$.

In the bottom-tier transmission process, an actuator may be potentially within the transmission range of multiple ADs.[3] Therefore, each actuator could be cooperatively served by a cluster of selected ADs with joint beamforming, which is beneficial for increasing the strength of received signal. Let $\mathbf{h}_m \in \Re^{S\times 1}$ and $\mathbf{w}_m \in \Re^{1\times S}$ denote the channel state information vector and network-wide transmit beamformer vector from single-antenna ADs to actuator m, respectively. $\mathbf{h}_{m,n} \in \Re^{S\times 1}$ is the unit-power interference to actuator m when all single-antenna ADs transmitting the data for actuator n. With the linear transmit beamforming scheme at the AD, the signal to interference plus noise ratio (SINR) of signal received by actucator m is given by

$$\Gamma_m^b = \frac{\mathbf{w}_m \mathbf{h}_m \mathbf{h}_m^* \mathbf{w}_m^*}{\sum_{n\neq m, n\in\mathcal{M}} \mathbf{w}_n \mathbf{h}_{m,n} \mathbf{h}_{m,n}^* \mathbf{w}_n^* + \sigma_m^b}, \quad (9)$$

where σ_m^b is the receive noise power at actuator m. The available bandwidth for ADs is F_b that would be reused by all actuators, where $F_b = F - F_t$ and $F_t = |\mathcal{K}_m|\Delta F$. Thus, the achievable sum rate of each actuator is given by $R_m^b(\mathbf{w}_m) = F_b \log(1 + \Gamma_m^b)$. We note that the bandwidth allocation between the top-tier and bottom-tier transmissions is conflict. In other words, if too many bandwidths are assigned to the top-tier transmission process, the bottom-tier transmission will be the bottleneck, i.e., many data packets would be dropped at ADs. On the contrary, if too many bandwidths are assigned to the bottom-tier transmission process, the transmission capacity in the top tier is limited, which would reduce the success probability $\Pr\{R_{m,s}^t(\mathbf{v}, \mathbf{a}) \geq R_{th}^t\}$. The lower the success probability is, the fewer the number of ADs that decode data packets successfully is. It means that the cooperation gain achieved by spatial diversity is lower and the top-tier transmission is the bottleneck. Therefore, there exists a trade-off between the top-tier and bottom-tier transmissions to maximize the end-to-end transmission reliability as well as the spectrum efficiency and energy efficiency.

The joint beamforming has ability to enhance the SINR of received signal and transmission reliability via prop-

[3]For the frequency and phase synchronization problem [39], this paper adopts the master-slave open-loop synchronization method. According to the hierarchical architecture considered in this paper, for the master-slave frequency synchronization, the remote controller acts as the master and all ADs are designed as the slaves. In this paper, we focus on the transmission scheduling scheme design (networking protocol) to alleviate the impact of unreliable wireless transmission on the control performance with the assumption on perfect synchronization.

$$\mu_{m,t} \geq \frac{\mathbb{E}\{(\mathbf{x}_t^m)^{\mathrm{T}}[(A_m)^{\mathrm{T}}U_m A_m - \eta_m L_m]\mathbf{x}_t^m\}}{\mathbb{E}\{(\mathbf{x}_t^m)^{\mathrm{T}}[(A_m)^{\mathrm{T}}U_m A_m - (A_m - B_m G_m)^{\mathrm{T}}U_m(A_m - B_m G_m)]\mathbf{x}_t^m\}} \tag{5}$$

$$\max_{\{\mathbf{x}_t^m \neq \mathbf{0}\}} \frac{\mathbb{E}\{(\mathbf{x}_t^m)^{\mathrm{T}}[A_m^{\mathrm{T}}U_m A_m - \eta_m U_m]\mathbf{x}_t^m\}}{\mathbb{E}\{(\mathbf{x}_t^m)^{\mathrm{T}}[A_m^{\mathrm{T}}U_m A_m - (A_m - B_m G_m)^{\mathrm{T}}U_m(A_m - B_m G_m)]\mathbf{x}_t^m\}} \tag{6}$$

erly designing the beamforming vector. The instantaneous adaptation of the beamformer and power is possible to optimize the SNR in (8) and/or the SINR in (9) for each actuator. However, each receiver will have to sense the channel state over time in an active way. This will lead to a huge amount of feedback overhead and energy consumption and in general is not easy to implement in practice. In this paper, the outage probability is used to evaluate the transmission performance [40]. In this way, the instantaneous channel state information does not need to be known, instead, the channel distribution information is necessary. The outage probability of m-th actuator's data packet delivered by the remote controller via selected ADs is $\Pr\{R_m^b(\mathbf{w}_m) < R_{th}^b\}$, which indicates that the coordinated single-antenna ADs forming a virtual multi-antenna array has superiority on enhancing the throughput and transmission quality. Taking the power limitation into account, $\sum_{m\in\mathcal{M}} (\mathbf{w}_m(s))^2 \leq P_s$, where the constant P_s denotes the maximum transmission power of AD s, and $\mathbf{w}_m(s)$ denotes the s-th element of the vector $\mathbf{w}_m$.

In order to make full utilization of limited spectrum and energy resources, in next section, we will investigate how to jointly optimize the control law and the transmission strategy to minimize the weighted sum of energy consumption and control cost under the condition of system stability.

IV. Joint Optimization of Control Scheduling and Transmission Strategy

As mentioned above, the control command and the transmission reliability jointly determine the system stability and the objective function of formulated problem. Thus, it is of importance to optimize the joint design of control scheduling and transmission strategy for the multi-subsystem WCS to minimize the overall cost. However, the tight coupling between two designs makes it challenging to find out the optimal solution. Fortunately, the control law could be calculated quickly, meaning that the computation cycle is much less than the communication cycle. Therefore, we firstly calculate the control law, and then schedule the control commands through wireless transmissions, which makes it possible to obtain a suboptimal solution effectively by separating the control and transmission designs.

Note that for a single time step $t \in [0, T]$, the control input $\mathbf{u}_t^m$ depends only on the current state $\mathbf{x}_t^m$ and all previous transmissions/controls ($\beta_{m,t'}, \mathbf{u}_{t'}^m, t' \in [0, t-1]$). It means that the current transmission $\beta_{m,t}$ has no impact on the current control input $\mathbf{u}_t^m$, but affects the next-step control input $\mathbf{u}_{t+1}^m$. In this case, we propose to design the control and transmission strategies in sequence. In particular, the control decision is made firstly, and then optimize the transmission design based on channel conditions, system dynamics and control decisions. For the transmission design at step t, all previous transmissions/controls and current control input are regarded fixed variables, and the improvement of transmission performance can only be achieved by adjusting the free variables (such as beam, power and channel). Therefore, the control design could be separated from the transmission strategy design, and the transmission design should be aware of the control design and system dynamics.

For the subsystem $m \in \mathcal{M}$, the control command executed by actuator is $\check{\mathbf{u}}_{m,t} = \beta_{m,t}\mathbf{u}_{m,t}$, and the expected linear-quadratic loss of the closed-loop system $\Delta\mathcal{J}_m$ is defined as

$$\begin{aligned}\Delta\mathcal{J}_m &= \mathbb{E}\Big\{\sum_{t=0}^{T-1}(\mathbf{u}_t^m - \check{\mathbf{u}}_t^m)^{\mathrm{T}} Q_m^u (\mathbf{u}_t^m - \check{\mathbf{u}}_t^m)\Big\} \\ &= \mathbb{E}\Big\{\sum_{t=0}^{T-1}(1-\beta_{m,t})(\mathbf{x}_t^m)^{\mathrm{T}} G_m^{\mathrm{T}} Q_m^u G_m \mathbf{x}_t^m (1-\beta_{m,t})\Big\}.\end{aligned} \tag{10}$$

Let $\mathcal{J}_{m,t}^Q = (\mathbf{x}_t^m)^{\mathrm{T}} G_m^{\mathrm{T}} Q_m^u G_m \mathbf{x}_t^m$, then

$$\Delta\mathcal{J}_m = \mathbb{E}\Big\{\sum_{t=0}^{T-1}(1-\beta_{m,t})^2 \mathcal{J}_{m,t}^Q\Big\} = \sum_{t=0}^{T-1}\mathbb{E}\Big\{(1-\beta_{m,t})^2\mathcal{J}_{m,t}^Q\Big\}.$$

For a single time step $t \in [0, T]$, the control input $\check{\mathbf{u}}_t^m = \beta_{m,t} G_m \mathbf{x}_t^m$ depends only on the current state $\mathbf{x}_t^m$ and the current transmission $\beta_{m,t}$. As the random variable $\beta_{m,t}$ and the random variable $\mathbf{x}_t^m$ are independent, $\mathbb{E}\big\{(1-\beta_{m,t})^2\mathcal{J}_{m,t}^Q\big\}$ is equivalent to $\mathbb{E}\big\{(1-\beta_{m,t})^2\big\}\mathbb{E}\big\{\mathcal{J}_{m,t}^Q\big\}$. Recalling that $\beta_{m,t}$ follows the Bernoulli distribution, we have $\mathbb{E}\{(1-\beta_{m,t})^2\} = 1 - \mathbb{E}\{\beta_{m,t}\}$. It thus follows that

$$\begin{aligned}\mathbb{E}\big\{(1-\beta_{m,t})^2\mathcal{J}_{m,t}^Q\big\} &= \mathbb{E}\big\{(1-\beta_{m,t})^2\big\}\mathbb{E}\big\{\mathcal{J}_{m,t}^Q\big\} \\ &= (1-\mathbb{E}\{\beta_{m,t}\})\mathbb{E}\big\{\mathcal{J}_{m,t}^Q\big\},\end{aligned} \tag{11}$$

and then

$$\begin{aligned}\Delta\mathcal{J}_m &= \sum_{t=0}^{T-1}\mathbb{E}\Big\{(1-\beta_{m,t})^2\mathcal{J}_{m,t}^Q\Big\} \\ &= \sum_{t=0}^{T-1}\big(1-\mathbb{E}\{\beta_{m,t}\}\big)\mathbb{E}\big\{\mathcal{J}_{m,t}^Q\big\},\end{aligned} \tag{12}$$

where the expectation is given by $\mathbb{E}\{(1-\beta_{m,t})^2\} = 1 - \mathbb{E}\{\beta_{m,t}\} = 1 - (1\cdot\Pr\{R_m^b(\mathbf{w}_m) \geq R_{th}^b\} + 0\cdot\Pr\{R_m^b(\mathbf{w}_m) < R_{th}^b\}) = 1 - \Pr\{R_m^b(\mathbf{w}_m) \geq R_{th}^b\}$.

As the optimization objective function involves time-varying variable $\mathbf{x}$ subject to time step t, we formulate the optimization

problem for each time t to guarantee the system stability and reduce the overall cost.

$$\mathcal{P}_0: \min_{\{\mathbf{v},\mathbf{w},\mathbf{a}\}} \sum_{m=1}^{M}\big(1-\Pr\{R_m^b(\mathbf{w}_m)\geq R_{th}^b\}\big)\mathbb{E}\{\mathcal{J}_m^Q\} + \varpi\Big(\sum_{m\in\mathcal{M}}\|\mathbf{w}_m\|_2^2+\sum_{k\in\mathcal{K}}\|\mathbf{v}[k]\|^2\Big) \tag{13}$$

$$\text{s.t. } \Pr\{R_m^b(\mathbf{w}_m)\leq R_{m,s}^t(\mathbf{v},\mathbf{a})\}\geq 1-\epsilon,$$

$$\forall m\in\mathcal{M},\quad \forall s\in\mathcal{S}_m, \tag{13a}$$

$$\sum_{m\in\mathcal{M}} a_m[k]\leq 1,\quad \forall k\in\mathcal{K}, \tag{13b}$$

$$\sum_{s\in\mathcal{S}}\sum_{k\in\mathcal{K}}\|\mathbf{v}_s[k]\|_2^2\leq P_C, \tag{13c}$$

$$\sum_{m\in\mathcal{M}}(\mathbf{w}_m(s))^2\leq P_s,\quad \forall s\in\mathcal{S}, \tag{13d}$$

$$\Pr\{R_m^b(\mathbf{w}_m)\geq R_{th}^b\}\geq\mu_{m,t}^{low},\quad \forall m\in\mathcal{M}, \tag{13e}$$

where the subscript t of $\beta_{m,t}$ and $\mathcal{J}_{m,t}^Q$ is omitted for notation simplicity; (13a) denotes the probability constraint on the relative relationship of achievable transmission rate between the top-tier and bottom-tier processes[45]; (13b) indicates that in the top-tier, a channel can be used to deliver data packets for at most one actuator; (13c) and (13d) are the transmission power constraints of remote controller and each AD, respectively; (13e) denotes the stability condition of each subsystem with intermittent control commands.

It is noted that (13a) is the only constraint relating the top-tier transmission and bottom-tier transmission, which can be regarded as the transmission ability of the top-tier process that is lower bounded by the bottom-tier one. This inspires us to obtain a sub-optimal solution of the original problem $\mathcal{P}_0$ by decomposing it into two subproblems. One focuses on the bottom-tier transmission optimization while the other aims to optimize the top-tier transmission. However, even for subproblems, the objective function, the constraint expressed in the implicit probabilistic form, and the coupling of binary variables and continuous variables make it challenging to obtain the optimal solutions.

A. Bottom-Tier Transmission Optimization

We note that the bandwidth allocation between the top-tier and bottom-tier transmissions is conflict. In other words, if too many bandwidths are assigned to the top-tier transmission process, the bottom-tier transmission will be the bottleneck, i.e., many data packets would be dropped at ADs. In order to mitigate the dropping packets problem, actuators would be more prone to selecting a part of ADs with better channel conditions, rather than putting all ADs into its candidate set $\mathcal{S}_m$. On the contrary, if only few ADs are selected, the top-tier transmission would be the bottleneck, making the cooperation gain achieved by spatial diversity lower and the end-to-end transmission quality worse. Therefore, there exists an optimal set of selected ADs (denoted as $\mathcal{S}_m^*\subset\mathcal{S}$) to maximize the end-to-end transmission reliability as well as the spectrum efficiency and energy efficiency.

In the dynamics aware transmission strategy, the remote controller delivers the data packet of actuator m to the set of ADs providing services for it (denoted as $\mathcal{S}_m=\{s\in\mathcal{S}:\Pr\{R_{m,s}^t(\mathbf{v},\mathbf{a})\geq R_{th}^t\}\geq\mu_{m,t}^{low},\mathbf{w}_m(s)>0,m\in\mathcal{M}\}$). The set $\mathcal{S}_m$ is a function of the optimization variables $\mathbf{w}$, $\mathbf{v}$ and $\mathbf{a}$ in the two-tier transmission process. As the set $\mathcal{S}_m$ determined by the decoding state of each AD during the top-tier transmission process could not be known aforehand, an indicator variable is introduced to clearly express the relationship between the set $\mathcal{S}_m$ and the decoding state in the top-tier transmission process. In particular,

$$\mathbb{1}_{\hat{\mathcal{S}}_m}(s)=\begin{cases}1, & \text{if } s\in\hat{\mathcal{S}}_m,\\ 0, & \text{if } s\notin\hat{\mathcal{S}}_m,\end{cases} \tag{14}$$

where $\hat{\mathcal{S}}_m=\{s\in\mathcal{S}:\Pr\{R_{m,s}^t(\mathbf{v},\mathbf{a})\geq R_{th}^t\}\geq\mu_{m,t}^{low},\ m\in\mathcal{M}\}$. Then the optimal set $\mathcal{S}_m^*$ is mathematically expressed as $S_m^*=\{s\in\mathcal{S}:\mathbb{1}_{\hat{\mathcal{S}}_m}(s)\cdot\mathbf{w}_m^*(s)>0,m\in\mathcal{M}\}$, where the optimal $\mathbf{w}_m^*(s)$ can be obtained by solving the following optimization problem.

$$\mathcal{P}_{\mathcal{S}}: \min_{\{\mathbf{v},\mathbf{w},\mathbf{a}\}} \sum_{m=1}^{M}\Big(1-\Pr\big\{R_m^b(\tilde{\mathbf{w}}_m)\geq R_{th}^b\big\}\Big)\mathbb{E}\big\{\mathcal{J}_m^Q\big\} + \varpi\Big(\sum_{s\in\mathcal{S}}\Big[\sum_{m\in\mathcal{M}}(\tilde{\mathbf{w}}_m(s))^2+\sum_{k\in\mathcal{K}}\big\|\mathbf{v}_s[k]\big\|_2^2\Big]\Big) \tag{15}$$

$$\text{s.t. } \Pr\{R_m^b(\tilde{\mathbf{w}}_m)\leq R_{m,s}^t(\mathbf{v},\mathbf{a})\}\geq 1-\epsilon, \tag{15a}$$

$$\forall m\in\mathcal{M},\quad \forall s\in\mathcal{S}, \tag{15b}$$

$$\sum_{m\in\mathcal{M}} a_m[k]\leq 1,\quad \forall k\in\mathcal{K}, \tag{15c}$$

$$\sum_{s\in\mathcal{S}}\sum_{k\in\mathcal{K}}\big\|\mathbf{v}_s[k]\big\|_2^2\leq P_C, \tag{15d}$$

$$\sum_{m\in\mathcal{M}}(\tilde{\mathbf{w}}_m(s))^2\leq P_s,\quad \forall s\in\mathcal{S}, \tag{15e}$$

$$\Pr\big\{R_m^b(\tilde{\mathbf{w}}_m)\geq R_{th}^b\big\}\geq\mu_{m,t}^{low},\quad \forall m\in\mathcal{M}, \tag{15f}$$

where $\tilde{\mathbf{w}}_m(s)=\mathbb{1}_{\hat{\mathcal{S}}_m}(s)\cdot\mathbf{w}_m(s)$, $\tilde{\mathbf{w}}_m=\mathbf{w}_m\otimes\mathbf{I}_{\hat{\mathcal{S}}_m}$ and $\mathbf{I}_{\hat{\mathcal{S}}_m}=[\mathbb{1}_{\hat{\mathcal{S}}_m}(1),\cdots,\mathbb{1}_{\hat{\mathcal{S}}_m}(s),\cdots,\mathbb{1}_{\hat{\mathcal{S}}_m}(S)]$.

Based on the result in [41] and [42, Th. 1], the constraint (15e) expressed in an implicit probabilistic form can be transformed to an explicit deterministic expression. In particular, as we consider the outage probability as a performance index due to the random channels, the instantaneous channel state information is not needed. Instead, the channel distribution information is used to reduce the feed back information when channel changes. The random variable $\mathbf{h}_m$ is considered to follow a complex-normal distribution, i.e., $\text{vec}(\mathbf{h}_{m,n})\sim CN(0,\Sigma_{m,n})$, where the channel covariance

[4] In the two-tier communication architecture, the achievable rate in the bottom-tier process is upper bounded by that in the top-tier process, expressed by (13a). In the worse case that the data volume received by actuators in the unit transmission duration is smaller than the packet size of control command, the constraint (13e) can not satisfied. In this regard, the event that the achievable transmission rate of top-tier process is less than that of bottom-tier process, will induce the negative impact on control stability and system performance. Due to the randomness of top-tier and bottom-tire transmission rates, the probability that the above event occurs is upper bounded by a small and acceptable threshold ϵ.

[5] If in the time division duplex mode, the condition (13a) is modified to $\Pr\{R_m^b(\mathbf{w}_m)\leq R_{m,s}^t(\mathbf{v},\mathbf{a})\cdot\frac{T_t}{T_b}\}\geq 1-\epsilon$.

matrices $\Sigma_{m,n}$'s are determined by the channel distribution information and vec$(\cdot)$ is the vectorization expression of a matrix. Then, outage probability $\Pr\{R_m^b(\tilde{\mathbf{w}}_m) \geq R_{th}^b\}$ can be rewritten as

$$\Pr\Big\{\frac{\tilde{\mathbf{w}}_m \mathbf{h}_m \mathbf{h}_m^* \tilde{\mathbf{w}}_m^*}{\sum\limits_{n\neq m, n\in\mathcal{M}} \tilde{\mathbf{w}}_n \mathbf{h}_{m,n} \mathbf{h}_{m,n}^* \tilde{\mathbf{w}}_n^* + \sigma_m^b} \geq \Gamma_{th}^b\Big\} = \exp\Big(-\frac{\Gamma_{th}^b \sigma_m^b}{c_m p_m}\Big) \prod_{n\neq m, n\in\mathcal{M}} \big(1 + \frac{\Gamma_{th}^b c_m^n p_n}{c_m p_m}\big)^{-1}, \quad (16)$$

where $\Gamma_{th}^b = \exp\big(\frac{R_{th}^b \ln 2}{F_b}\big) - 1$ is a positive constant related to the given bandwidth F_b. In addition, $c_m = \frac{\tilde{\mathbf{w}}_m}{|\tilde{\mathbf{w}}_m|} \mathbf{\Sigma}_{m,m} \frac{\tilde{\mathbf{w}}_m^*}{|\tilde{\mathbf{w}}_m^*|}$, $c_m^n = \frac{\tilde{\mathbf{w}}_n}{|\tilde{\mathbf{w}}_n|} \mathbf{\Sigma}_{m,n} \frac{\tilde{\mathbf{w}}_n^*}{|\tilde{\mathbf{w}}_n^*|}$, $p_m = |\tilde{\mathbf{w}}_m|^2$ and $p_n = |\tilde{\mathbf{w}}_n|^2$. Based on (16), (13e) is reformed as

$$\frac{\Gamma_{th}^b \sigma_m^b}{c_m p_m} + \sum_{n\neq m, n\in\mathcal{M}} \ln\big(1 + \frac{\Gamma_{th}^b c_m^n p_n}{c_m p_m}\big) \leq -\ln(\mu_{m,t}^{low}) \quad (17)$$

Then the optimization problem of the bottom-tier transmission process is transformed to a static one, as shown in (18),

$$\mathcal{P}_{s_b}: \min_{\{\tilde{\mathbf{w}}\}} \sum_{m=1}^{M} -\mathbb{E}\{\mathcal{J}_m^Q\} \exp\Big(-\frac{\Gamma_{th}^b \sigma_m^b}{c_m p_m}\Big) \times \prod_{n\neq m, n\in\mathcal{M}} \big(1 + \frac{\Gamma_{th}^b c_m^n p_n}{c_m p_m}\big)^{-1} + \mathbb{E}\{\mathcal{J}_m^Q\} + \varpi \sum_{m\in\mathcal{M}} \big\|\tilde{\mathbf{w}}_m\big\|_2^2 \quad (18)$$

$$\text{s.t. C1:} \sum_{m\in\mathcal{M}} (\tilde{\mathbf{w}}_m(s))^2 \leq P_s, \quad \forall s \in \mathcal{S} \quad (19)$$

$$\text{C2:} \frac{\Gamma_{th}^b \sigma_m^b}{c_m p_m} + \sum_{n\neq m, n\in\mathcal{M}} \ln\big(1 + \frac{\Gamma_{th}^b c_m^n p_n}{c_m p_m}\big) \leq -\ln(\mu_{m,t}^{low}), \quad \forall m \in \mathcal{M} \quad (20)$$

The solution of problem $\mathcal{P}_{s_b}$ could be obtained by solving $\mathcal{P}_{s_b}^c$ and $\mathcal{P}_{s_b}^p$ in sequence. In particular, $\mathcal{P}_{s_b}^c$ takes charge of the beamformer design with normalized transmission power, which is optimally solved with the golden section method. $\mathcal{P}_{s_b}^c$ performs the power control with given beamformer, whose suboptimal solution is easily obtained by solving an equation set with the quasi-Newton method. See Appendix A for the detailed solution process.

B. Top-Tier Transmission Optimization

In this subsection, we firstly deal with the constraint expressed in the implicit probabilistic form. As the optimization problem of the top-tier transmission is mixed-integer programming, it is difficult to solve it directly. We solve the channel allocation problem and the beamformer design problem, respectively.

1) Transformation of the Expression in Probabilistic Form: With the obtained $\tilde{\mathbf{w}}$, the value of $R_m^b(\mathbf{w}_m)$ in expectation can be calculated by letting $\mathbf{w} = \tilde{\mathbf{w}}$, shown as below.

$$\overline{R}_m^b(\mathbf{w}_m) = F_b \log(1 + \frac{\mathbf{w}_m^* \mathbf{\Sigma}_{m,m} \mathbf{w}_m}{\sum\limits_{n\neq m, n\in\mathcal{M}} \mathbf{w}_m^* \mathbf{\Sigma}_{m,n} \mathbf{w}_n + \sigma_m^b}). \quad (21)$$

The decoding state of the top-tier process can be determined by the beamforming vector $\mathbf{w}$ of the bottom-tier transmission process. In this regard, the relationship between the set $\mathcal{S}_m$ and the beamforming vector $\mathbf{w}$ is

$$\mathbb{1}\{(\mathbf{w}_m(s))^2\} = \begin{cases} 1, \text{ if } (\mathbf{w}_m(s))^2 > 0 \\ 0, \text{ if } (\mathbf{w}_m(s))^2 = 0, \end{cases} \quad (22)$$

Thus, $\mathcal{S}_m$ can be determined by the obtained solution $\mathbf{w}$, i.e., $\mathcal{S}_m = \{s \in \mathcal{S} : \mathbb{1}\{(\mathbf{w}_m(s))^2\} > 0, m \in \mathcal{M}\}$. In order to overcome the difficulty caused by the objective function in probabilistic form, the difference-convex programming is employed to reformulate (13a),

$$\Pr\{R_{m,s}^t \geq \overline{R}_m^b(\mathbf{w}_m)\} \geq 1 - \epsilon, \quad \forall s \in \mathcal{S}_m \Rightarrow \mathbb{E}\big\{\mathbb{1}\{D_{m,s}^t\}\big\} \geq 1 - \epsilon, \quad \forall s \in \mathcal{S}, \quad (23)$$

where $D_{m,s}^t = R_{m,s}^t(\mathbf{v}, \mathbf{a}) - R_m^b(\mathbf{w}_m) \cdot \mathbb{1}\{(\mathbf{w}_m(s))^2\}$. Thus (13a) is approximated to

$$\max_{s\in\mathcal{S}} \exp\big(-\mathbb{E}\{D_{m,s}^t\}/\varrho\big) \leq \epsilon, \quad (24)$$

where $\mathbb{E}\{D_{m,s}^t\} = \overline{R}_{m,s}^t(\mathbf{v}, \mathbf{a}) - \overline{R}_m^b(\mathbf{w}_m) \cdot \mathbb{1}\{(\mathbf{w}_m(s))^2\}$ and $\overline{R}_{m,s}^t = \sum\limits_{k\in\mathcal{K}} a_m[k] \Delta F \log(1 + \frac{1}{\sigma_s^t[k]} \mathbb{E}\{\mathbf{v}_s[k] \mathbf{g}_s[k] \mathbf{g}_s^*[k] \mathbf{v}_s^*[k]\})$. The expectation $\mathbb{E}\{\mathbf{g}_s[k]\mathbf{g}_s^*[k]\}$ is the integral of random vector $\mathbf{g}_s[k]$ that denotes the complex channel gain from the control to the s-th AD on the k-th channel. Based on the result in [41] and [42, Th. 1], the random variable $\mathbf{g}_s[k]$ follows a complex-normal distribution, i.e., $\mathbf{g}_s[k] \sim CN(0, \Xi_s[k])$, where the channel covariance $\Xi_s[k]$'s are determined by the channel distribution information. See Appendix B for the detailed derivation of (24). The optimization problem of the top-tier transmission process is expressed as

$$\mathcal{P}_{s_t}: \min_{\{\mathbf{v},\mathbf{a}\}} \varpi \sum_{s\in\mathcal{S}_m} \Big\{\sum_{k\in\mathcal{K}} \big\|\mathbf{v}_s[k]\big\|^2 + \exp\big(-\mathbb{E}\{D_{m,s}^t\}/\varrho\big) \mathbb{E}\big\{\mathcal{J}_m^Q\big\}\Big\}$$
$$\text{s.t. } \exp\big(-\mathbb{E}\{D_{m,s}^t\}/\varrho\big) \leq \epsilon, \quad \forall s \in \mathcal{S}, \text{ (13b), (13c),}$$

which is mix-integer programming. In general, it's not easy to solve it with low complexity, we seek to obtain a sub-optimal solution instead.

2) Channel Allocation for the Data Transmission From the Remote Controller to ADs: For notation simplicity, let $\mathcal{K}_m \triangleq \{k \in \mathcal{K} : a_m[k] = 1\}$ denote the channels allocated to transmit the control command packet of actuator m. Then we consider how to determine the binary variable $\mathbf{a}$ with given set $\mathcal{K}_m$. The main idea of Algorithm 1 is that $\exp\big(-\mathbb{E}\{D_{m,s}^t\}/\varrho\big)$ is proportional to the channel condition $\Xi_s[k]$. We sort all channels in the non-increasing order of $\Xi_s[k]$ for each actuator as well as all actuators in the non-increasing order of $\mathcal{J}_m^Q$. Then the first actuator selects the favorite channel (i.e. $a_m[k] = 1$ and $a_{m'}[k] = 0, m' \neq m$). Other actuators select their own most favorite channel in sequence. If the most favorite channel has been selected by others, the actuator will select next channel in order. Until all actuators have selected one channel, the value

of $\exp\big(-\mathbb{E}\{D^t_{m,s}\}/\varrho\big)\mathbb{E}\big\{\mathcal{J}^Q_m\big\}$ is then used to re-arrange all actuators in descending order until all channels have been occupied.

Algorithm 1 Heuristic Algorithm to Determine the Channel Allocation Variable $\mathbf{a}$

1: **Input:** Channel condition indicator $\Xi_s[k]$ and execution derivation $\mathbb{E}\big\{\mathcal{J}^Q_m\big\}$;
2: **Output:** Channel allocation status $\mathbf{a}$;
3: **Initialize:** Preference factors of each subsystem and channel are $\upsilon_m = \mathbb{E}\big\{\mathcal{J}^Q_m\big\}$ and $\omega[k] = \Xi_s[k]$, respectively;
4: **for** each subsystem/actuator $m \in \mathcal{M}$ **do**
5: Sort all subsystem in the non-increasing order with respect to υ_m, and the ordered set is $\hat{\mathcal{M}}$;
6: **for** each channel $k \in \mathcal{K}_m$ **do**
7: Sort all channels in the nonincreasing order with respect to $\omega[k]$, and the ordered set is $\hat{\mathcal{K}}_m$;
8: **end for**
9: **end for**
10: **repeat**
11: $m^* = \arg\max_{m\in\hat{\mathcal{M}}} \upsilon_m$ and $\hat{\mathcal{M}} = \hat{\mathcal{M}} \setminus m^*$;
12: Subsystem m^* selects the first channel in the ordered set $\hat{\mathcal{K}}_m$, i.e., $k^* = \arg\max_{k\in\hat{\mathcal{K}}_m} \omega[k]$;
13: $a_{m^*}[k^*] = 1$ and $a_m[k^*] = 0, m \neq m^*, m \in \mathcal{M}$;
14: Remove the selected channel k^* from set $\hat{\mathcal{K}}_m$ for all subsystems, i.e., $\hat{\mathcal{K}}_m = \hat{\mathcal{K}}_m \setminus k^*, \forall m \in \hat{\mathcal{M}}$;
15: **until** $\{\mathcal{K}_m = \emptyset$ or $\hat{\mathcal{M}} = \emptyset$ $\}$
16: **while** $\mathcal{K}_m \neq \emptyset$ **do**
17: $\check{\upsilon}_m = \exp\big(-\mathbb{E}\{D^t_{m,s}\}/\varrho\big)\mathbb{E}\big\{\mathcal{J}^Q_m\big\}$;
18: Sort all subsystem in the non-increasing order with respect to the value of $\check{\upsilon}_m$, and the ordered set is $\check{\mathcal{M}}$;
19: Step 11 - Step 14;
20: **end while**
21: Return the channel allocation status $\mathbf{a}$.

The computational complexity of Algorithm 1 contains three aspects: sorting the set elements, searching the set elements and executing the looping statements. The complexity of sorting subsystems (Step 5) and channels (Step 7) are $\mathcal{O}(|\mathcal{M}|\log(|\mathcal{M}|))$ and $\mathcal{O}(|\mathcal{K}|\log(|\mathcal{K}|))$. For each relay, the complexity of selecting the best actuator (Step 11) and searching the best channel for the selected actuator (Step 12) are $\mathcal{O}(|\mathcal{M}|)$ and $\mathcal{O}(|\mathcal{K}|)$, respectively. In the worst case, only one channel could been determined in one iteration, and there are $|\mathcal{K}|$ iterations at most. Therefore, the computational complexity of Algorithm 1 is $\mathcal{O}(|\mathcal{K}|(\mathbb{N}\log(\mathbb{N}) + \mathbb{N}))$, which is no more than $\mathcal{O}(\mathbb{N}^2\log(\mathbb{N}))$, where $\mathbb{N} = \max\{|\mathcal{M}|, |\mathcal{K}|\}$.

3) Beamformer Design: After obtaining the sets $\mathcal{K}_m$ and $\mathcal{S}_m$, the problem can be modified as

$$\begin{aligned}
&\mathcal{P}'_{s_t}: \\
&\min_{\{\mathbf{v}\}} \ \varpi \sum_{s\in\mathcal{S}_m}\sum_{k\in\mathcal{K}_m} \big\|\mathbf{v}_s[k]\big\|_2^2 + \exp\big(-\mathbb{E}\{\tilde{D}^t_{m,s}\}/\varrho\big)\mathbb{E}\big\{\mathcal{J}^Q_m\big\} \\
&\text{s.t. } \exp\big(-\mathbb{E}\{\tilde{D}^t_{m,s}\}/\varrho\big) \le \epsilon, \quad \forall s \in \mathcal{S}_m, \ \forall k \in \mathcal{K}_m, \\
&\qquad \sum_{s\in\mathcal{S}_m}\sum_{k\in\mathcal{K}_m} \big\|\mathbf{v}_s[k]\big\|_2^2 \le P_C,
\end{aligned}$$

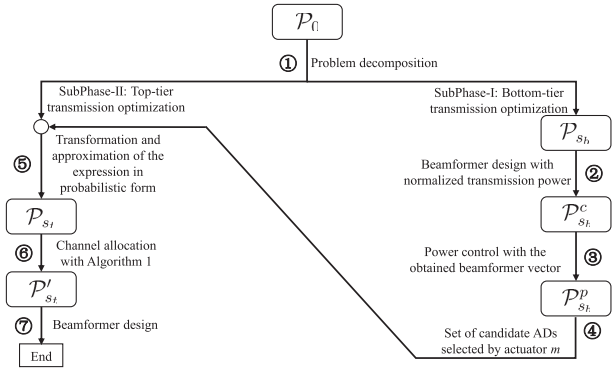

Fig. 2. Flowchart of the problem-solving process.

where $\mathbb{E}\{\tilde{D}^t_{m,s}\} = \sum_{k\in\mathcal{K}_m} \Delta F \log(1 + \frac{\mathbf{v}^*_s[k]\Xi_s[k]\mathbf{v}_s[k]}{\sigma^t_s[k]})$. It is easy to verify that the left-hand side of the first constraint monotonically increases with the reduction of $\big\|\mathbf{v}_s[k]\big\|_2^2$. This means that the value of $\big\|\mathbf{v}_s[k]\big\|_2^2$ can not be too small to satisfy this constraint. The minimum value can be reached when $\exp\big(-\mathbb{E}\{\tilde{D}^t_{m,s}\}/\varrho\big) = \epsilon$, which is regarded as one extreme point. The other extreme point can be gotten by letting the first-order derivative of $\mathcal{P}'_{s_t}$ be equal to zero. Comparing the two extreme points, the one with the smallest function value is selected as the solution of $\mathcal{P}'_{s_t}$.

In short, the original problem $\mathcal{P}_0$ could be solved effectively by firstly solving the $\mathcal{P}_{s_b}$ subproblem and then the $\mathcal{P}_{s_t}$ subproblem. Fig. 2 shows the flowchart of the problem-solving process. In particular, based on the interrelationship between bottom-tier and top-tier transmissions, the sub-optimal solution of original problem $\mathcal{P}_0$ is obtained by decomposing it into two subproblems. One focuses on the bottom-tier transmission optimization while the other aims to optimize the top-tier transmission. Both the differential accumulation and the difference-convex methods are employed to effectively deal with the constraint expressed in the implicit probabilistic form. Then, the bottom-tier optimization subproblem is solved sub-optimally by dealing with the beamformer design with normalized transmission power and the power control with given beamformer sequentially. For the top-tier optimization subproblem, its suboptimal solution could be obtained by dealing with the channel allocation and beamformer design sequentially. As the former is a 0-1 integer programming, the Algorithm 1 is designed to get suboptimal solutions in polynomial time.

V. Simulation Results

The hot rolling process in the iron and steel industry is regarded as a typical process control system in the industrial IoT, where the physical components are constituted of five main stages, i.e., waling beam furnace, reversing rougher, finishing mill, laminar cooling and down coilers, as shown in Fig. 3. In this paper, we consider the temperature control in the laminar cooling stage. The slab temperature is measured by sensors and then deliver to the remote controller. Based on the received temperature measurements, the controller determines the control commands for different control subsystems.

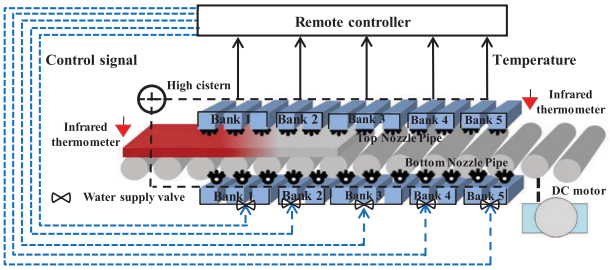

Fig. 3. Laminar cooling stage.

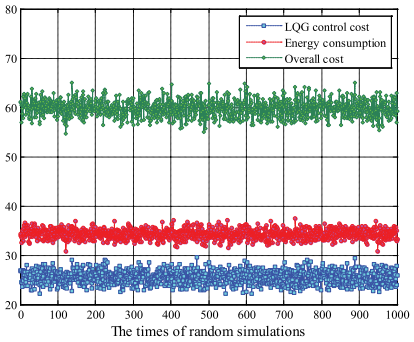

Fig. 4. Performance of DACT scheme.

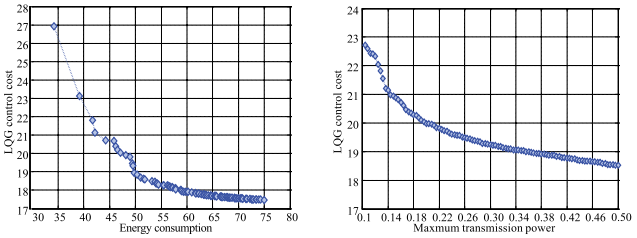

(a) Control cost vs. energy consumption (b) Control cost vs. power budget

Fig. 5. Tradeoff between control cost and energy consumption.

The calculated control commands are delivered to actuators via shared wireless channels, and the valves of nozzles are adjusted based on received control commands to control the slab temperature to a target region.

In each subsystem, the valves of nozzles are adjusted based on control commands to control the slab temperature to a specific value. The discrete-time linear model for the m-th subsystem can be expressed by

$$\mathbf{x}_{t+1}^m = A_m \mathbf{x}_t^m + B_m \mathbf{u}_t^m + \zeta_t^m,$$

where $\mathbf{x}_t^m$ is the state vector of slab's temperature and $B_m = \text{diag}\{1, 0, \cdots, 0, 1\}_{\kappa_x \times \kappa_u}$. According to [34], $A_m = \text{diag}\{A_{1,m}, A_{2,m}, A_{3,m}, A_{4,m}\}$ is given by (25),

$$A_{r,m} = \text{diag}\{\frac{\mathcal{T}\Delta t \varpi^{1,r,m}}{\Delta b^2 \varsigma^{1,r,m} c^{1,r,s}}, \frac{\mathcal{T}\Delta t \varpi^{2,r,m}}{\Delta b^2 \varsigma^{2,r,m} c^{2,r,m}}, \frac{\mathcal{T}\Delta t \varpi^{3,r,m}}{\Delta b^2 \varsigma^{3,r,m} c^{3,r,m}}, \frac{\mathcal{T}\Delta t \varpi^{4,r,m}}{\Delta b^2 \varsigma^{4,r,m} c^{4,r,m}}\} \times \begin{bmatrix} -2 & 2 & 0 & 0 \\ 1 & -2 & 1 & 0 \\ 0 & 1 & -2 & 1 \\ 0 & 0 & 2 & -2 \end{bmatrix} + I, \quad (25)$$

where $r = \{1, 2, 3, 4\}$, slab thermal conductivity $\varpi = 40W/mK$, slab density $\varsigma = 7.85kg/m^3$, slab specific heat capacity $c = 0.46 \times 103J/kg \cdot K$, and slab thickness $\Delta b = 1/2m$.

In simulations, we adopt an empirical industrial wireless channel model in the physical layer [43], which consists of a large-scale path loss, a shadow fading and a small-scale.

$$PL(d) = PL_0 + 10n \log_{10}(d/d_0) + \kappa, \quad (26)$$

where $PL_0 = 56.7$dB is the path loss at the reference distance $d_0 = 1$m [44], $n = 4.31$ is the path loss exponent [45], and the shadowing coefficient $\kappa = 6$dB is zero-mean Gaussian distributed random variable in dB with standard deviation $\sigma = -87$dBm [46].

A. Performance Evaluation

In this subesection, we evaluate the performance of proposed dynamics-aware and beamforming-assisted coordinated transmission (abbreviated as DACT) strategy in terms of overall cost, estimation error and energy consumption, respectively. Each metric is obtained by performing 1000 independent simulation trials. An example (random realization) of the considered multi-subsystem WCS consists of one remote controller with 8 antennas, 10 subsystems and 15 ADs, simulation result is shown as Fig. 4. It is seen that the overall cost consistes of two major components, and then we will discuss the tradeoff between control cost and energy consumption, as shown as Fig. 5. In Fig. 5(a), it can be seen that the LQG control cost decreases with the increasing of energy consumption, when the maximum transmission power is given. Therefore, for a given transmission power budget, there exists a point that achieves the minimum sum of control cost and energy consumption. Fig. 5(b) shows the relationship between control cost and maximum transmission power (i.e. the maximum tolerant energy consumption) of remote controller. The LQG control cost reduces with the growth of transmission power budget, meaning that there is a transmission power budget that could achieve the minimum sum of control cost and energy consumption. Based on the aforementioned discussions, it can be derived that there is a tradeoff between control cost and energy consumption to minimize the overall cost of WCSs.

B. Performance Comparison

For a fair comparison, the following transmission strategies are introduced.

- PACT: Packet-loss aware actuator-centric transmission strategy aims to reduce the packet loss rate of control commands with the frequency-diversity based multicast beamforming technique, but without taking the system dynamics into account.
- DBT: Dynamics driven broadcast-based transmission aims to reduce the overall system cost, which is achieved through broadcasting all control comments to all ADs,

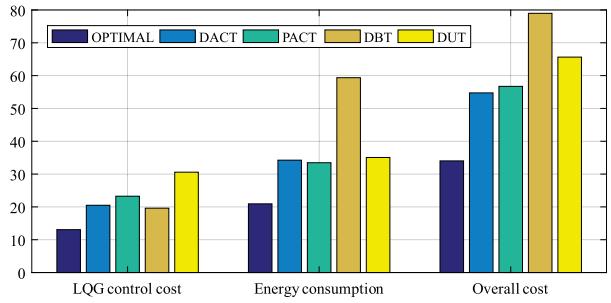

Fig. 6. Performance comparison among the optimal solution and four different strategies.

and then ADs forward the decoded information to actuators in a coordinated way.

- DUT: Dynamics driven unicast-based transmission aims to reduce the overall system cost under the condition of given matching relationship between ADs and actuators. Moreover, one actuator can be served by only one AD and the remote controller delivers the control comments to corresponding AD with single spatial stream on different channels.

We evaluate the performances of DACT, PACT, DBT and DUT strategies in terms of overall cost, estimation error and energy consumption, respectively. The gap between the optimal solution and the sub-optimal one obtained with the DACT strategy is shown as Fig. 6. The mix-integer programming in the top-tier transmission are optimally solved with the brute-force method. The optimal set of selected assisted devices and the two-tier transmission parameters are obtained with the exhaustive search method. Fig. 6 shows that the proposed DACT strategy achieves the lowest control-communication overall cost. For the performance of control cost, DACT, PACT and DBT strategies are much better than the DUT strategy, reducing about 33%, 23%, and 34%, respectively. This is because that the coordination among multiple ADs is able to considerably decrease the mutual interference and improve the transmission reliability. Note that DBT strategy has the best performance in term of control cost, but this is achieved at the cost of a great deal of energy consumption. The reason is that the multicast transmission can save more energy than the broadcoast one, especially when the channel conditions of a few controller-AD pairs are bad. DACT strategy has ability to provide better control performance than PACT strategy, even though the caused energy consumption with DACT and PACT strategies are similar. The reason is that PACT strategy decides the transmission strategy based on only the wireless communication environment without considering the dynamics of control system. In fact, different control subsystems have distinct dynamics, thus successfully delivering control commands for different subsystems would get different contributions on improving the control performance of the whole system. For multi-subsystem WCSs, it is necessary to take both channel condition and system dynamics into the account of transmission strategy design. At the same time, it is also of significant importance

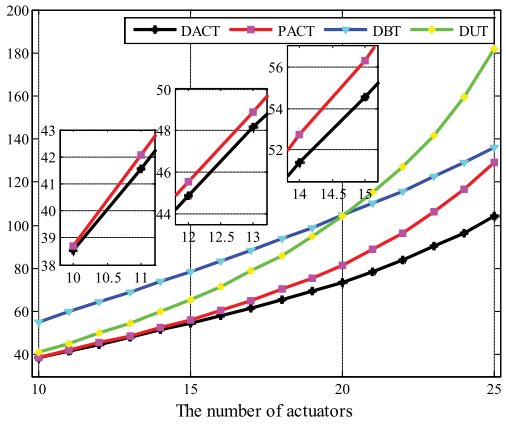

(a) Overall cost comparison

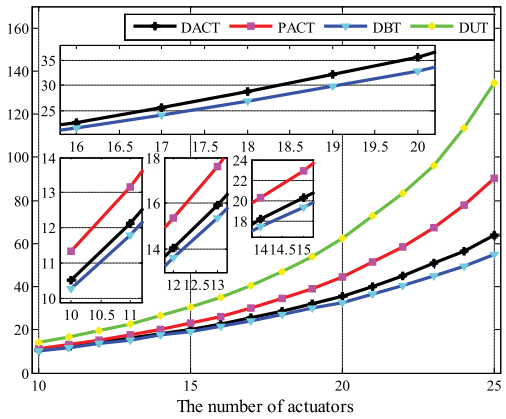

(b) LQG control cost comparison

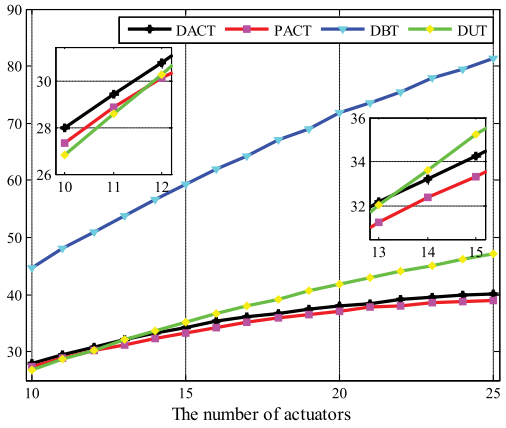

(c) Energy consumption comparison

Fig. 7. Performance comparison among four strategies with different numbers of actuators.

to consider the joint optimization of transmission strategy and control law for multi-subsystem WCSs.

In order to show the impact of different system parameters on strategy performance, such as the number of actuators and the number of ADs, we compare the four strategies by fixing one variable and changing the other one. Note that each result in Fig. 7 and Fig. 8 is achieved by averaging 100 runs of the algorithms over randomly generated channels. With the change of the number of actuators and ADs, four strategies have similar performance in terms of overall cost, control cost and energy consumption. Fig. 7 shows that the

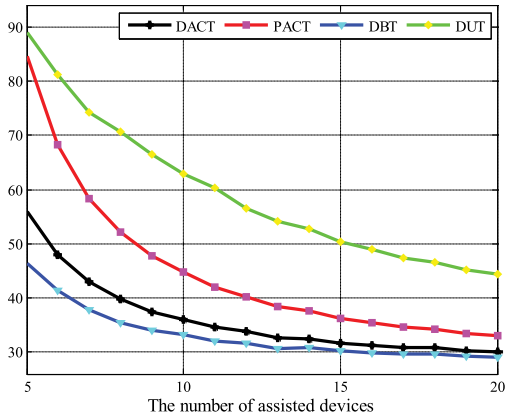

(a) LQG control cost comparison

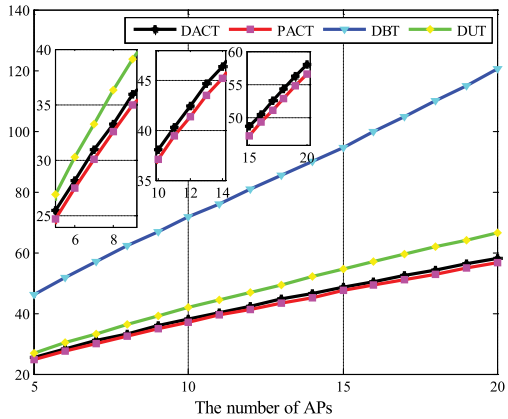

(b) Energy consumption comparison

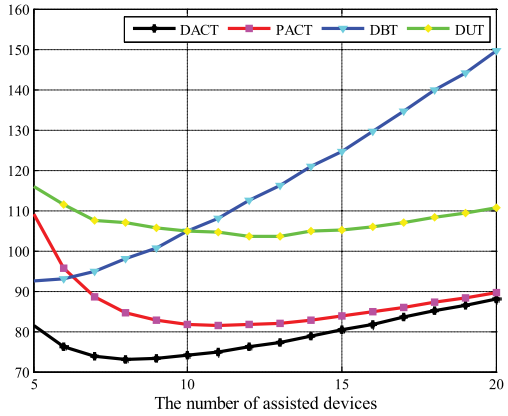

(c) Overall cost comparison

Fig. 8. Performance comparison among four strategies with different numbers of assisted devices.

values of considered three performance metrics increase with the number of actuators. Therefore, the larger the system is, the higher the execution cost is. In addition, it can be seen that the overall cost of DACT strategy is always smaller than others, meaning that the proposed DACT strategy has higher scalability than others. Fig. 8(a) shows that the control cost decreases with the number of ADs, since the larger number of ADs could provide the higher space diversity and increase the transmission reliability. Fig. 8(b) shows that the energy consumption increases with the growth of the number of ADs. The overall cost achieved with DACT, PACT and DUT strategies drops at the beginning and then rises later, shown as Fig. 8(c). In a short, Fig. 8 shows that it is not quite reasonable to achieve a better possible overall performance for multi-subsystem WCSs by increasing the number of ADs.

VI. Conclusions

The multi-subsystem WCSs with intermittent control commands caused by limited and lossy wireless channels have been investigated in this paper. We have explored the relationship between control performance and transmission quality, based on which, a dynamics-aware and beamforming-assisted transmission strategy has been proposed for control scheduling. Simulation results have demonstrated that the designed DACT strategy has the advantage to reduce the overall cost than other strategies without awareness of system dynamics. Moreover, the joint design of transmit beamforming and power control not only achieves a significant improvement on the energy efficiency, but also has a good adaptivity to the system dynamics and channel conditions. For future work, we will investigate the joint design of cooperative transmission and coordination control for the WCS with multiple coupled subsystems, especially in large-scale control systems.

Appendix A
Detailed Solution Process of (18)

The solution of problem $\mathcal{P}_{s_b}$ is obtained by solving $\mathcal{P}^c_{s_b}$ and $\mathcal{P}^p_{s_b}$ in sequence. For each AD s, $p_m(s) = |\tilde{\mathbf{w}}_m(s)|^2$, the projection of unit-norm vectors $\frac{\tilde{\mathbf{w}}^*_m}{|\tilde{\mathbf{w}}^*_m|}$ on the channel gain vector $\mathbf{h}_m$ are $c_m(s) = \frac{\tilde{\mathbf{w}}_m}{|\tilde{\mathbf{w}}_m|}(s)\mathbf{\Sigma}_{m,m}\frac{\tilde{\mathbf{w}}_m}{|\tilde{\mathbf{w}}_m|}(s)$ and $c^n_m(s) = \frac{\tilde{\mathbf{w}}_n}{|\tilde{\mathbf{w}}_n|}(s)\mathbf{\Sigma}_{m,n}\frac{\tilde{\mathbf{w}}^*_n}{|\tilde{\mathbf{w}}^*_n|}(s)$, respectively. Then, the objective function of $\mathcal{P}_{s_b}$ is rewritten as

$$\sum\nolimits_{m=1}^{M} -\mathcal{J}^Q_m \exp\left(-\mathcal{L}_m\right) + \mathcal{J}^Q_m + \varpi \sum_{m\in\mathcal{M}}\sum_{s\in\mathcal{S}} p_m(s), \quad (27)$$

where $\mathcal{L}_m = \sum_{n\neq m, n\in\mathcal{M}} \ln\left(1 + \frac{\Gamma^b_{th}\sum_{s\in\mathcal{S}} p_n(s)c^n_m(s)}{\sum_{s\in\mathcal{S}} p_m(s)c_m(s)}\right) + \frac{\Gamma^b_{th}\sigma^b_m}{\sum_{s\in\mathcal{S}} p_m(s)c_m(s)}$. As the logarithm operation does not change the monotonicity, we then focus on getting the optimal $c_m(s)$ and $c^n_m(s)$ in terms of minimizing $\mathcal{L}_m$. The beamformer design with given transmission power can be obtained by solving $\mathcal{P}^c_{s_b}$,

$$\mathcal{P}^c_{s_b}: \min_{\{\mathbf{c}\}} \sum_{m=1}^{M} \mathcal{L}_m, \quad \text{s.t. } 0 \le \mathcal{L}_m \le -\ln(\mu^{low}_{m,t}), \quad \forall m \in \mathcal{M}. \quad (28)$$

The first-order derivatives of $\mathcal{L}_m$ with respect to $c_m(s)$ and $c^n_m(s)$ are

$$\frac{\partial \mathcal{L}_m}{\partial c^n_m(s)} = \frac{\Gamma^b_{th} p_m(s)}{\Gamma^b_{th}\sum_{s\in\mathcal{S}} p_m(s)c^n_m(s) + \sum_{s\in\mathcal{S}} p_m(s)c_m(s)} > 0, \quad (29)$$

$$\frac{\partial \mathcal{L}_m}{\partial c_m(s)} = \frac{\sum_{s\in\mathcal{S}} p_m(s)c_m(s)}{\Gamma^b_{th}\sum_{s\in\mathcal{S}} p_m(s)c^n_m(s) + \sum_{s\in\mathcal{S}} p_m(s)c_m(s)}$$

$$\times \frac{-\Gamma_{th}^{b}\sum\limits_{s\in\mathcal{S}} p_m^2(s)c_m^n(s)}{\big(\sum\limits_{s\in\mathcal{S}} p_m(s)c_m(s)\big)^2} + \frac{-\Gamma_{th}^{b}\sigma_m^b p_m(s)}{\big(\sum\limits_{s\in\mathcal{S}} p_m(s)c_m(s)\big)^2} < 0, \tag{30}$$

which indicates that $\mathcal{L}_m$ (the objective function of $\mathcal{P}_{s_b}^{c}$) monotonically decreases with $c_m(s)$, but monotonically increases with $c_m^n(s)$. Note that, $c_m(s)$ cannot be infinitely large and $c_m(s)$ and $c_m^n(s)$ cannot be infinitely small, since $\mathcal{L}_m$ are bounded by constraint (20). According to the monotonicity, the optimal $c_m(s)$ could be obtained with the golden section method in the feasible area, when $c_m^n(s)$ is given. Similarly, the optimal $c_m^n(s)$ could be obtained, when the $c_m(s)$ is given. With the given beamformer $\tilde{\mathbf{c}}$, the power control problem is formulated as below.

$$\begin{aligned}\mathcal{P}_{s_b}^{p}:\ \min_{\{\mathbf{p}\}}\ & \varpi\sum_{m\in\mathcal{M}}\sum_{s\in\mathcal{S}} p_m(s)\\ \text{s.t.}\ & \sum_{n\neq m, n\in\mathcal{M}} \ln\Big(1+\frac{\Gamma_{th}^{b}\sum\limits_{s\in\mathcal{S}} p_m(s)\tilde{c}_m^n(s)}{\sum\limits_{s\in\mathcal{S}} p_m(s)\tilde{c}_m(s)}\Big)\\ & + \frac{\Gamma_{th}^{b}\sigma_m^b}{\sum\limits_{s\in\mathcal{S}} p_m(s)\tilde{c}_m(s)} \le -\ln(\mu_{m,t}^{low}),\quad \forall m\in\mathcal{M},\\ & \sum_{m\in\mathcal{M}} p_m(s)\tilde{c}_m(s)\le P_s,\quad \forall s\in\mathcal{S},\end{aligned} \tag{31}$$

whose minimum value can be reached when $\sum\limits_{n\neq m, n\in\mathcal{M}} \ln\big(1+\frac{\Gamma_{th}^{b}\sum\limits_{s\in\mathcal{S}} p_m(s)\tilde{c}_m^n(s)}{\sum\limits_{s\in\mathcal{S}} p_m(s)\tilde{c}_m(s)}\big) + \frac{\Gamma_{th}^{b}\sigma_m^b}{\sum\limits_{s\in\mathcal{S}} p_m(s)\tilde{c}_m(s)} = -\ln(\mu_{m,t}^{low})$. Then the optimal transmission power $\mathbf{p}^*$ for all ADs is obtained. In this way, the solution of problem $\mathcal{P}_{s_b}$ is obtained by solving $\mathcal{P}_{s_b}^{c}$ and $\mathcal{P}_{s_b}^{p}$ in sequence.

APPENDIX B
DERIVATION OF (24)

In (23), $D_{m,s}^t = R_{m,s}^t - R_m^b\cdot\mathbb{1}\{(\mathbf{w}_m(s))^2\}$. In addition, $\mathbb{1}\{\min\limits_{s\in\mathcal{S}} D_{m,s}^t\} = 1$, if $\min\limits_{s\in\mathcal{S}} D_{m,s}^t \ge 0$. Otherwise, $\mathbb{1}\{\min\limits_{s\in\mathcal{S}} D_{m,s}^t\} = 0$. It worth noting that the indicator function can be equivalently expressed with the ℓ_0-norm. However, ℓ_0-norm is still intractable since it is a discontinuous function. We use the scheme proposed by Rinaldi [35] to approximate the ℓ_0-norm,

$$\begin{aligned}\mathbb{E}\big\{\mathbb{1}\{\min_{s\in\mathcal{S}} D_{m,s}^t\}\big\} &= \mathbb{1}\big\{\min_{s\in\mathcal{S}}\mathbb{E}\{D_{m,s}^t\}\big\} = \|\min_{s\in\mathcal{S}}\mathbb{E}\{D_{m,s}^t\}\|_0\\ &\approx 1-\exp\Big(-\frac{\min\limits_{s\in\mathcal{S}}\mathbb{E}\{D_{m,s}^t\}}{\varrho}\Big),\end{aligned} \tag{32}$$

where $\mathbb{E}\{D_{m,s}^t\} = \sum\limits_{k\in\mathcal{K}} a_m[k]\Delta F\log\big(1+\frac{\mathbf{v}_s^*[k]\Xi_s[k]\mathbf{v}_s[k]}{\sigma_s^t[k]}\big) - \overline{R}_m^b\cdot\mathbb{1}\{(\mathbf{w}_m(s))^2\}$. It can be observed that

$$\lim_{\varrho\to 0}\exp\Big(-\frac{\min\limits_{s\in\mathcal{S}}\mathbb{E}\{D_{m,s}^t\}}{\varrho}\Big) = \begin{cases}1, & \text{if } \min\limits_{s\in\mathcal{S}}\mathbb{E}\{D_{m,s}^t\}=0\\ 0, & \text{if } \min\limits_{s\in\mathcal{S}}\mathbb{E}\{D_{m,s}^t\}\neq 0,\end{cases}$$

which could be approximated to

$$\exp\Big(-\frac{\min\limits_{s\in\mathcal{S}}\mathbb{E}\{D_{m,s}^t\}}{\varrho}\Big)\approx\begin{cases}1, & \text{if } \min\limits_{s\in\mathcal{S}}\mathbb{E}\{D_{m,s}^t\}\ll\frac{\varrho}{2}\\ 0, & \text{if } \min\limits_{s\in\mathcal{S}}\mathbb{E}\{D_{m,s}^t\}\gg\frac{\varrho}{2},\end{cases} \tag{33}$$

where ϱ is the smoothing parameter determining the quality of the approximation [47]. The approximation in (32) and (33) tends to equality, when $\varrho\to 0$. Thus, (13a) is approximated to

$$\max_{s\in\mathcal{S}}\exp\big(-\mathbb{E}\{D_{m,s}^t\}/\varrho\big)\le\epsilon. \tag{34}$$

REFERENCES

[1] C. Chen, J. Yan, N. Lu, Y. Wang, X. Yang, and X. Guan, "Ubiquitous monitoring for industrial cyber-physical systems over relay-assisted wireless sensor networks," *IEEE Trans. Emerg. Topics Comput.*, vol. 3, no. 3, pp. 352–362, Sep. 2015.

[2] N. Cheng, N. Lu, N. Zhang, T. Yang, X. Shen, and J. W. Mark, "Vehicle-assisted device-to-device data delivery for smart grid," *IEEE Trans. Veh. Technol.*, vol. 65, no. 4, pp. 2325–2340, Apr. 2016.

[3] L. Lyu, C. Chen, C. Hua, S. Zhu, and X. Guan, "Co-design of stabilisation and transmission scheduling for wireless control systems," *IET Control Theory Appl.*, vol. 11, no. 11, pp. 1767–1778, 2017.

[4] H. Zhang *et al.*, "Scheduling with predictable link reliability for wireless networked control," *IEEE Trans. Wireless Commun.*, vol. 16, no. 9, pp. 6135–6150, Sep. 2017.

[5] L. Lyu, C. Chen, S. Zhu, N. Cheng, and X. Shen, "Demand-driven and energy-efficient transmission for multi-loop wireless control systems," in *Proc. IEEE Int. Conf. Commun.*, May 2018, pp. 1–6.

[6] N. Zhang *et al.*, "Software defined networking enabled wireless network virtualization: Challenges and solutions," *IEEE Netw.*, vol. 31, no. 5, pp. 42–49, May 2017.

[7] H. Guo, J. Ren, D. Zhang, Y. Zhang, and J. Hu, "A scalable and manageable IoT architecture based on transparent computing," *J. Parallel Distrib. Comput.*, vol. 118, pp. 5–13, Aug. 2018, doi: 10.1016/j.jpdc.2017.07.003.

[8] L. Lyu, C. Chen, S. Zhu, and X. Guan, "5G enabled codesign of energy-efficient transmission and estimation for industrial IoT systems," *IEEE Trans. Ind. Informat.*, vol. 14, no. 6, pp. 2690–2704, Jun. 2018, doi: 10.1109/TII.2018.2799685.

[9] P. Chen and Q. L. Han, "On designing a novel self-triggered sampling scheme for networked control systems with data losses and communication delays," *IEEE Trans. Ind. Electron.*, vol. 63, no. 2, pp. 1239–1248, Feb. 2016.

[10] C. Ramesh, H. Sandberg, and K. H. Johansson, "Design of state-based schedulers for a network of control loops," *IEEE Trans. Autom. Control*, vol. 58, no. 8, pp. 1962–1975, Aug. 2013.

[11] S. Zhu, C. Chen, W. Li, B. Yang, and X. Guan, "Distributed optimal consensus filter for target tracking in heterogeneous sensor networks," *IEEE Trans. Cybern.*, vol. 43, no. 6, pp. 1963–1976, Dec. 2013.

[12] H. Zhang, L. Li, J. Xu, and M. Fu, "Linear quadratic regulation and stabilization of discrete-time systems with delay and multiplicative noise," *IEEE Trans. Autom. Control*, vol. 60, no. 10, pp. 2599–2613, Oct. 2015.

[13] A. Molin and S. Hirche, "Price-based adaptive scheduling in multi-loop control systems with resource constraints," *IEEE Trans. Autom. Control*, vol. 59, no. 12, pp. 3282–3295, Dec. 2014.

[14] S. Zhu, C. Chen, X. Ma, B. Yang, and X. Guan, "Consensus based estimation over relay assisted sensor networks for situation monitoring," *IEEE J. Sel. Topics Signal Process.*, vol. 9, no. 2, pp. 278–291, Mar. 2015.

[15] M. C. F. Donkers, W. P. M. H. Heemels, N. van de Wouw, and L. Hetel, "Stability analysis of networked control systems using a switched linear systems approach," *IEEE Trans. Autom. Control*, vol. 56, no. 9, pp. 2101–2115, Sep. 2011.

[16] X. Cao, X. Zhou, L. Liu, and Y. Cheng, "Energy-efficient spectrum sensing for cognitive radio enabled remote state estimation over wireless channels," *IEEE Trans. Wireless Commun.*, vol. 14, no. 4, pp. 2058–2071, Apr. 2015.

[17] L. Zhang and D. Hristu-Varsakelis, "Communication and control co-design for networked control systems," *Automatica*, vol. 42, no. 6, pp. 953–958, Jun. 2006.

[18] S.-L. Dai, H. Lin, and S. S. Ge, "Scheduling-and-control codesign for a collection of networked control systems with uncertain delays," *IEEE Trans. Control Syst. Technol.*, vol. 18, no. 1, pp. 66–78, Jan. 2010.
[19] K. Gatsis, M. Pajic, A. Ribeiro, and G. J. Pappas, "Opportunistic control over shared wireless channels," *IEEE Trans. Autom. Control*, vol. 60, no. 12, pp. 3140–3155, Dec. 2015.
[20] S. Al-Areqi, D. Görges, and S. Liu, "Event-based networked control and scheduling codesign with guaranteed performance," *Automatica*, vol. 57, pp. 128–134, Jul. 2015.
[21] V. C. Gungor and G. P. Hancke, "Industrial wireless sensor networks: Challenges, design principles, and technical approaches," *IEEE Trans. Ind. Electron.*, vol. 56, no. 10, pp. 4258–4265, Oct. 2009.
[22] L. Lei, Y. Kuang, X. S. Shen, K. Yang, J. Qiao, and Z. Zhong, "Optimal reliability in energy harvesting industrial wireless sensor networks," *IEEE Trans. Wireless Commun.*, vol. 15, no. 8, pp. 5399–5413, Aug. 2016.
[23] US D.O.E., "Industrial wireless technology for the 21st century," Technol. Foresight, Tech. Rep., 2004.
[24] M. A. Mahmood, W. K. G. Seah, and I. Welch, "Reliability in wireless sensor networks: A survey and challenges ahead," *Comput. Netw.*, vol. 79, pp. 166–187, Mar. 2015.
[25] Y. Sadi and S. C. Ergen, "Energy and delay constrained maximum adaptive schedule for wireless networked control systems," *IEEE Trans. Wireless Commun.*, vol. 14, no. 7, pp. 3738–3751, Jul. 2015.
[26] V. N. Swamy *et al.*, "Real-time cooperative communication for automation over wireless," *IEEE Trans. Wireless Commun.*, vol. 16, no. 11, pp. 7168–7183, Nov. 2017.
[27] Y. Jing and H. Jafarkhani, "Network beamforming using relays with perfect channel information," *IEEE Trans. Inf. Theory*, vol. 55, no. 6, pp. 2499–2517, Jun. 2009.
[28] Y. Huang, C. W. Tan, and B. D. Rao, "Joint beamforming and power control in coordinated multicell: Max-min duality, effective network and large system transition," *IEEE Trans. Wireless Commun.*, vol. 12, no. 6, pp. 2730–2742, Jun. 2013.
[29] S. He, Y. Huang, S. Jin, and L. Yang, "Coordinated beamforming for energy efficient transmission in multicell multiuser systems," *IEEE Trans. Commun.*, vol. 61, no. 12, pp. 4961–4971, Dec. 2013.
[30] J. Huang, P. Wang, and Q. Wan, "Collaborative beamforming for wireless sensor networks with arbitrary distributed sensors," *IEEE Commun. Lett.*, vol. 16, no. 7, pp. 1118–1120, Jul. 2012.
[31] K. Zarifi, S. Zaidi, S. Affes, and A. Ghrayeb, "A distributed amplify-and-forward beamforming technique in wireless sensor networks," *IEEE Trans. Signal Process.*, vol. 59, no. 8, pp. 3657–3674, Aug. 2011.
[32] D. Gündüz, E. Erkip, A. J. Goldsmith, and H. V. Poor, "Reliable joint source-channel cooperative transmission over relay networks," *IEEE Trans. Inf. Theory*, vol. 59, no. 4, pp. 2442–2458, Apr. 2013.
[33] D. Xue, Y. Chen, and D. P. Atherton, *Linear Feedback Control: Analysis and Design With MATLAB*. Philadelphia, PA, USA: SIAM, 2007.
[34] L. Lyu, C. Chen, J. Yan, F. Lin, C. Hua, and X. Guan, "State estimation oriented wireless transmission for ubiquitous monitoring in industrial cyber-physical systems," *IEEE Trans. Emerg. Topics Comput.*, to be published.
[35] J. Daafouz, P. Riedinger, and C. Iung, "Stability analysis and control synthesis for switched systems: A switched Lyapunov function approach," *IEEE Trans. Autom. Control*, vol. 47, no. 11, pp. 1883–1887, Nov. 2002.
[36] V. Gupta, B. Hassibi, and R. M. Murray, "Optimal LQG control across packet-dropping links," *Syst. Control Lett.*, vol. 56, no. 6, pp. 439–446, Jun. 2007.
[37] M. Grant and S. Boyd. *CVX: MATLAB Software for Disciplined Convex Programming, Version 2.1*. Accessed: Sep. 13, 2018. [Online]. Available: http://cvxr.com/cvx
[38] Z. K. Nagy and R. D. Braatz, "Open-loop and closed-loop robust optimal control of batch processes using distributional and worst-case analysis," *J. Process Control*, vol. 14, no. 4, pp. 411–422, 2004.
[39] R. Mudumbai, D. R. B. Iii, U. Madhow, and H. V. Poor, "Distributed transmit beamforming: Challenges and recent progress," *IEEE Commun. Mag.*, vol. 47, no. 2, pp. 102–110, Feb. 2009.
[40] N. Cheng *et al.*, "Performance analysis of vehicular device-to-device underlay communication," *IEEE Trans. Veh. Technol.*, vol. 66, no. 6, pp. 5409–5421, Jun. 2017.
[41] X. Zhai, C. W. Tan, Y. Huang, and B. D. Rao, "Transmit beamforming and power control for optimizing the outage probability fairness in MISO networks," *IEEE Trans. Commun.*, vol. 65, no. 2, pp. 839–850, Feb. 2017.
[42] S. Ghosh, B. D. Rao, and J. R. Zeidler, "Outage-efficient strategies for multiuser MIMO networks with channel distribution information," *IEEE Trans. Signal Process.*, vol. 58, no. 12, pp. 6312–6324, Dec. 2010.
[43] Y. Shi, J. Zhang, B. O'Donoghue, and K. B. Letaief, "Large-scale convex optimization for dense wireless cooperative networks," *IEEE Trans. Signal Process.*, vol. 63, no. 18, pp. 4729–4743, Sep. 2015.
[44] A. F. Molisch *et al.* (2004). *IEEE 802.15.4a Channel Model-Final Report*. [Online]. Available: http://www.ieee802.org/15/pub/TG4a.html
[45] Z. Irahhauten, G. J. M. Janssen, H. Nikookar, A. Yarovoy, and L. P. Ligthart, "UWB channel measurements and results for office and industrial environments," in *Proc. IEEE Int. Conf. Ultra-Wideband*, Waltham, MA, USA, Sep. 2006, pp. 225–230.
[46] E. Tanghe *et al.*, "The industrial indoor channel: Large-scale and temporal fading at 900, 2400, and 5200 MHz," *IEEE Trans. Wireless Commun.*, vol. 7, no. 7, pp. 2740–2751, Jul. 2008.
[47] Y.-F. Liu and Y.-H. Dai, "On the complexity of joint subcarrier and power allocation for multi-user OFDMA systems," *IEEE Trans. Signal Process.*, vol. 62, no. 3, pp. 583–596, Feb. 2014.

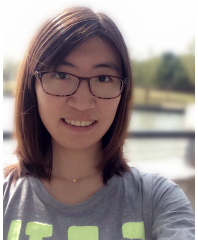

Ling Lyu (S'16) received the B.S. degree in telecommunication engineering from Jinlin University, Changchun, China, in 2013. She was a visiting student with the University of Waterloo, Canada, from 2017 to 2018. She is currently pursuing the Ph.D. degree with the Department of Automation, School of Electronic Information and Electrical Engineering, Shanghai Jiao Tong University, Shanghai, China. Her current research interests include wireless sensor and actuator network and application in industrial automation, the joint design of communication and control in industrial cyber-physical systems, estimation and control over lossy wireless networks, machine type communication enabled reliable transmission in the fifth generation network, resource allocation, and energy efficiency.

Cailian Chen (S'03–M'06) received the B.Eng. and M.Eng. degrees in automatic control from Yanshan University, China, in 2000 and 2002, respectively, and the Ph.D. degree in control and systems from the City University of Hong Kong, Hong Kong, in 2006. She was a Senior Research Associate with the City University of Hong Kong in 2006 and a Post-Doctoral Research Associate with The University of Manchester, U.K., from 2006 to 2008. She was a Visiting Professor with the University of Waterloo, Canada, from 2013 to 2014. She joined the Department of Automation, Shanghai Jiao Tong University, in 2008, as an Associate Professor, where she is currently a Full Professor.

She has worked actively on various topics such as wireless sensor networks and industrial applications, computational intelligence and distributed situation awareness, cognitive radio networks and system design, Internet of Vehicles and applications in intelligent transportation, and distributed optimization. She has authored and/or co-authored two research monographs and over 100 referred international journal and conference papers. She is the inventor of over 20 patents. She received the prestigious IEEE Transactions on Fuzzy Systems Outstanding Paper Award in 2008, and the Best Paper Award of The Ninth International Conference on Wireless Communications and Signal Processing in 2017. She received the First Prize of Natural Science Award twice from The Ministry of Education of China in 2006 and 2016, respectively. She was honored as a Changjiang Young Scholar by the Ministry of Education of China in 2015 and Excellent Young Researcher by the NSF of China in 2016.

Shanying Zhu (S'12–M'15) received the B.S. degree in information and computing science from the North China University of Water Resources and Electric Power, Zhengzhou, China, in 2006, the M.S. degree in applied mathematics from the Huazhong University of Science and Technology, Wuhan, China, in 2008, and the Ph.D. degree in control theory and control engineering from Shanghai Jiao Tong University, Shanghai, China, in 2013. From 2013 to 2015, he was a Research Fellow with the School of Electrical and Electronic Engineering, Nanyang Technological University, Singapore, and also with Berkeley Education Alliance for Research, Singapore. He joined Shanghai Jiao Tong University, in 2015, where he is currently an Associate Professor with the Department of Automation. His research interests focus on multi-agent systems and wireless sensor networks, particularly in coordination control of mobile robots and distributed detection and estimation in sensor networks and their applications in industrial network.

Nan Cheng (S'12–M'16) received the B.E. and M.S. degrees from the Department of Electronics and Information Engineering, Tongji University, Shanghai, China, in 2009 and 2012, respectively, and the Ph.D. degree from the Department of Electrical and Computer Engineering, University of Waterloo, in 2016. He was a Post-Doctoral Fellow with the Department of Electrical and Computer Engineering, University of Toronto, and also with the Department of Electrical and Computer Engineering, University of Waterloo under the supervision of Prof. B. Liang and Prof. S. Shen, from 2017 to 2018. He is currently a Professor with the School of Telecommunication Engineering, Xidian University, Shanxi, China. His current research focuses on space-air-ground integrated system, big data in vehicular networks, and self-driving system. His research interests also include performance analysis, MAC, opportunistic communication, and the application of AI for vehicular networks.

Yujie Tang (S'12) received the Ph.D. degree from the Department of Electrical and Computer Engineering, University of Waterloo, Canada. She is currently a Post-Doctoral Fellow with the Broadband Communications Research Group, University of Waterloo. Her research interests include vehicular ad hoc networks, software defined networks, machine learning, cognitive radio networks, cooperative networks, and resource management in heterogenous networks.

Xinping Guan (M'04–SM'04–F'18) is currently a Chair Professor with Shanghai Jiao Tong University, China, where he is also the Dean of the School of Electronic, Information and Electrical Engineering, and the Director of the Key Laboratory of Systems Control and Information Processing, Ministry of Education of China.

His current research interests include industrial cyber-physical systems, wireless networking and applications in smart city and smart factory, and underwater sensor networks. He has authored and/or co-authored four research monographs, over 270 papers in IEEE Transactions and other peer-reviewed journals, and numerous conference papers. As a principal investigator, he has finished/been working on many national key projects. He is the Leader of the Prestigious Innovative Research Team of the National Natural Science Foundation of China. He is an Executive Committee Member of the Chinese Automation Association Council and the Chinese Artificial Intelligence Association Council.

He received the Second Prize of National Natural Science Award of China in 2008, the First Prize of Natural Science Award from the Ministry of Education of China in 2006 and 2016, and the First Prize of Technological Invention Award of Shanghai Municipal, China, in 2017. He was a recipient of the IEEE Transactions on Fuzzy Systems Outstanding Paper Award in 2008. He is a National Outstanding Youth honored by NSF of China, Changjiang Scholar by the Ministry of Education of China, and State-level Scholar of New Century Bai Qianwan Talent Program of China.

Xuemin (Sherman) Shen (M'97–SM'02–F'09) received the Ph.D. degree in electrical engineering from Rutgers University, New Brunswick, NJ, USA, in 1990. He is currently a University Professor with the Department of Electrical and Computer Engineering, University of Waterloo, Waterloo, ON, Canada. His research focuses on resource management in interconnected wireless/wired networks, wireless network security, social networks, smart grid, and vehicular ad hoc and sensor networks. He is a registered Professional Engineer of Ontario, Canada, an Engineering Institute of Canada Fellow, a Canadian Academy of Engineering Fellow, a Royal Society of Canada Fellow, and a Distinguished Lecturer of the IEEE Vehicular Technology Society and Communications Society.

Dr. Shen received the James Evans Avant Garde Award from the IEEE Vehicular Technology Society, the Joseph LoCicero Award in 2015, and the Education Award in 2017 from the IEEE Communications Society. He has also received the Excellent Graduate Supervision Award in 2006 and the Outstanding Performance Award in 2004, 2007, 2010, and 2014 from the University of Waterloo, and the Premier's Research Excellence Award in 2003 from the Province of Ontario, Canada. He served as the Technical Program Committee Chair/Co-Chair for the IEEE Globecom 2016, the IEEE Infocom 2014, the IEEE VTC 2010 Fall, the IEEE Globecom 2007, the Symposia Chair for the IEEE ICC 2010, the Tutorial Chair for the IEEE VTC 2011 Spring, and the Chair for the IEEE Communications Society Technical Committee on Wireless Communications, and P2P Communications and Networking. He is the Editor-in-Chief of the IEEE INTERNET OF THINGS JOURNAL. He is the Vice President of Publications of the IEEE Communications Society.